THE VELOCITY MEASUREMENT BY LDV
AT THE SIMULATED PLATE FUEL ASSEMBLY

Tae Sung Ha

Dept of Eng. Physics, McMaster University, 1280 Main St. W. Hamilton, Ontario, Canada L8S 4L7: hats@mcmaster.ca

ABSTRACT

For a more accurate safety analysis for McMaster Nuclear Reactor (MNR), local velocity measurements in a mock-up of the 18-plate fuel assembly are conducted over the range of M=2.0kg/s to 5.0kg/s (u=0.59m/s to 1.48m/s). To enable the measurement of the mass flow distribution through the channels by Laser Doppler Velocimeter(LDV), the curved fuel plate assembly is modified to flat fuel plates. The experimental result shows that the velocity profile is fairly symmetric for the 1st channel to the 17th subchannel at its center. The velocity in the peripheral area is slightly decreased while that directly above the circular pipe is correspondingly increased due to the effect of blockage by the exit endfitting. The mass flow rate fraction is fairly well distributed from the 1st to the 9th channels; at the outmost channels (1st and 3rd subchannels) the flow is approximately 95~97% of the average channel flow and at the central channels (4th and 8th subchannels) the flow is about 102~105% of the average channel mass flow rate. It is shown that the measured mass flow distribution is consistent with the results of the numerical calculation except 1st and 17th channels.

1. Introduction

Adequate cooling of fuel in nuclear reactors has always been an important factor. The optimization of heat transfer from the fuel to heat exchangers through control of coolant behavior is economic common sense. However, much of the impetus behind studies in reactor thermal-hydraulics is from the safety standpoint: insufficient local or global cooling predispose the fuel to burn out, which may lead to structural damage, and subsequent leaching of radioactive fission products. Thus, several studies on the velocity information at the individual subchannel of McMaster Nuclear Reactor have been conducted by experimental measurement and numerical calculation [1][2][3][4]. The flow rate distribution at each subchannel of 18-plate fuel element was experimentally obtained by measuring pressure drop, but it couldn't give the precise local velocity in the subchannels because of the measurement difficulty from the geometrical complex of fuel element due to curved fuel plates. Also the mass flow rate at each subchannel was numerically calculated based on the assumption of sparse exit loss coefficient, K. Therefore, the exact velocity measurement in the subchannels is demandingly needed to understand the local flow, velocity profile, and mass flow distribution for modern safety analyses in recent years.

In this experiment, the velocity at the simulated 18-plate fuel element is measured by LDV. For the velocity measurement at the subchannels, the curved fuel plates are replaced by the straight-flat plates by maintaining same wetted perimeter and hydraulic diameter. The velocity measurement at 6 different local points at each subchannel from 1st to 9th channel is conducted over the range of M=2.0kg to 5.0kg/s. From the velocity data, the velocity profile is obtained at each subchannel. The mass flow rate is also calculated from the velocity profile at each subchannel. Its distribution across the subchannels is compared with previous experimental result and numerical result.

2. Experimental detail

The test loop, shown in Figure 1, consists of a circulating pump, an open surge water tank, a single straight 18-plate fuel simulator, a flow orifice, a electric heater, a cooling tap water loop, and flow control valve. The surge water tank is located to maintain a constant pressure in the flow channel. The circulating pump will deliver mass flow rate from 2kg/s up to 5kg/. The test loop piping is made from plastic pipes and fittings. The loop will be filled with de-ionized water and operated approximately at the experimental temperature, 30°C. The electric heater is used to heat the cold de-ionized water up to the experimental temperature, and the cooling tap water loop is intended to remove the pump heat and maintain the loop water at the desired temperature, 30°C.

The modified 18-plate fuel element is fabricated from 13mm thick acrylic (transparent plastic) sheet. The flat 16 fuel plates are made from 1.27mm thick flat aluminum plates instead of the real curved ones for the use of the LDV. The changes in the fuel element geometry are compensated by maintaining the same hydraulic diameter
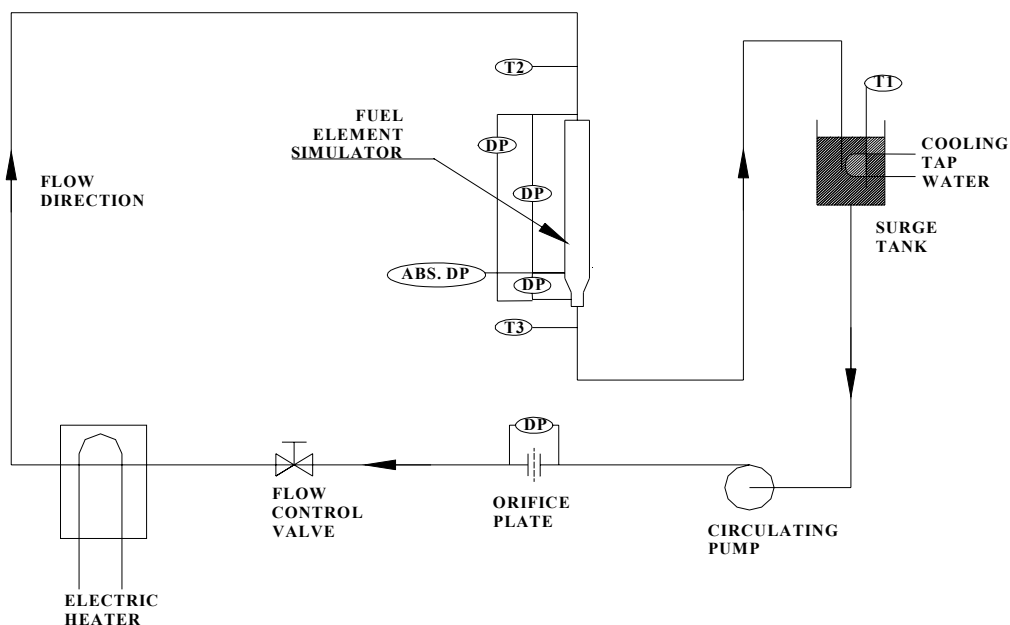
Figure 1. The loop schematic of MNR fuel assembly simulator

and wetted perimeter of the subchannels of the fuel element. The more detailed comparison of real 18-plate fuel element and simulated one is shown in Figure 2 and Table 1. The transition piece, which connects a rectangular channel with a round pipe bottom nozzle, is made from a cast Acrylic rod. The flow channel walls and the transition piece with a connecting flange is glued together using liquid cement.
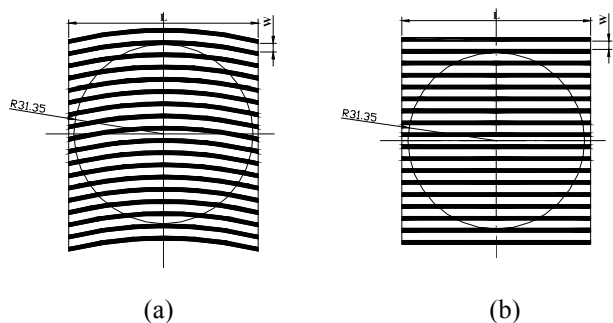

(a)   (b)

Figure 2. The comparison of real MNR fuel element with curve fuel plate (a) and simulated fuel element with straight flat aluminum plate (b)

The pressure transmitters measure the absolute pressure (ABS. DP) at test section and four differential pressures (DP): DP1 across the test section, DP2 across the end fitting of rectangular channel to circular pipe, and DP3 for DP1+DP2, and DP4 for the flow orifice as shown in Figure 1. They are selected for appropriate measurement pressure range depending on the pressure drop range and calibrated respectively.   The T-type thermocouples,

Table 1. The comparison of dimension of real MNR fuel element and simulated fuel element of 18-plate element

	Real MNR 18-plate fuel	Simulated 18-plate fuel
Length L[mm]	66.32	66.99
Width W[mm]	3.00	2.97
Cross-sectional area A [mm^2]	198.96	198.96
Wetted perimeter P [mm]	139.92	139.92
Hydraulic diameter D_h [mm]	5.6878	5.6878

which are verified by measuring the 0°C and 100°C with RTD for checking their correctness, are used for temperature measurements. The temperature at three different locations is measured: T1 at the surge tank, T2 at the upstream of test section, and T3 at the downstream of test section as shown in Figure 1. The flow velocities at the subchannel, entrance or exit flow are measured using LDV system. It consists of a 2 watt Lexel 95-2 Argon-Ion Laser unit, TSI transmitter optics (120, 250, and 600mm focal length), a TSI system 1980B signal processor, and a X-Y-Z (horizontal, vertical, and depth) traversing mechanism

with position locations. The velocity is measured at the center of each channel in X direction, six different locations in Y direction, and Z=1mm and Z=300mm in Z direction as shown in Figure 3. Vertically at each elevation, total 54 points' measurement are conducted and compared at each elevation. Here, the velocity profile in X direction is assumed symmetric because of geometrical symmetry as shown in Figure 2. Therefore the velocity only at a quarter of cross-sectional area in subchannels are measured; half cross-sectional area from 1st to 9th subchannels as shown in Figure 3 (b).
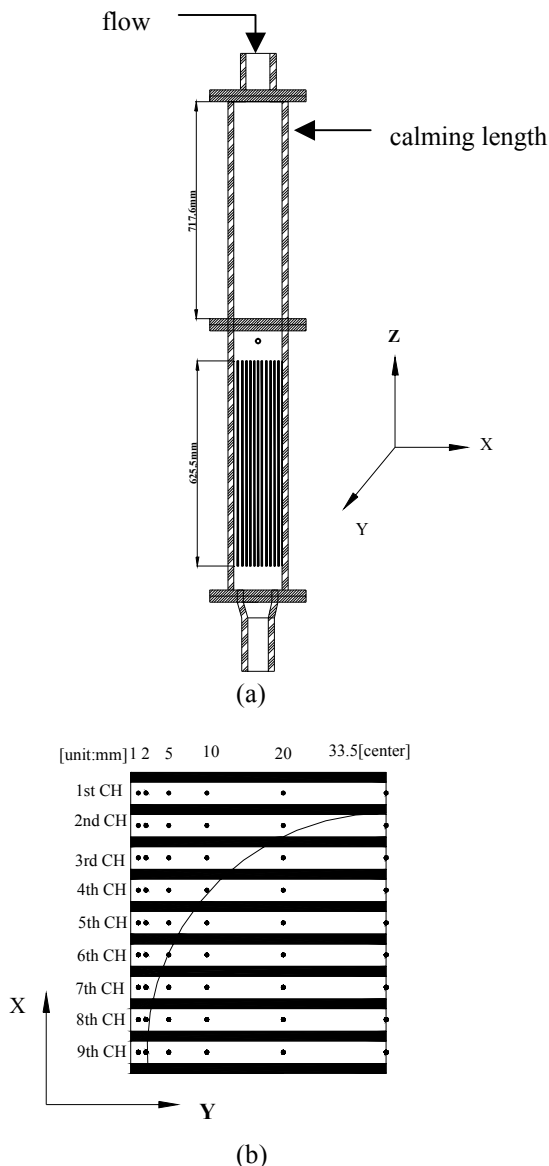

(a)

(b)

Figure 3. (a) The schematic of calming length and test section (b) the measurement point at ¼ cross-sectional area.

The individual instrument signals are connected via conditioning devices to a Digital Equipment Corporation (DEC) mini-computer basis data acquisition system. The temperature, mass flow rate, pressure drop, and velocity are updated by 5 seconds on the video screen. The steady-state data are recorded for a period of 100 seconds at a scanning rate of 10Hz. In this case, data points represent an average value of 1000 samples.

3. Result and Discussion

The mass flow rate and temperature of loop water are controlled during measurement by the controlling valve and cooling tap water, respectively. Typical result is shown in Figure 4 for M=3kg/s and T=30°C. Each data point presents about 1000 measurements' averaged value and total 54 points at different locations are shown. The standard deviation of mass flow rate and temperature are 0.34% and 7.46%, respectively. The mass flow rate is controlled very precisely while the temperature is fluctuating slightly because it is intended to control by cooling tap water within 30°C± 1°C. However, both are controlled fairly well. Therefore, the flow rate and fluid temperature throughout the measurement can be assumed constant; the water density variation during measurement is negligible.
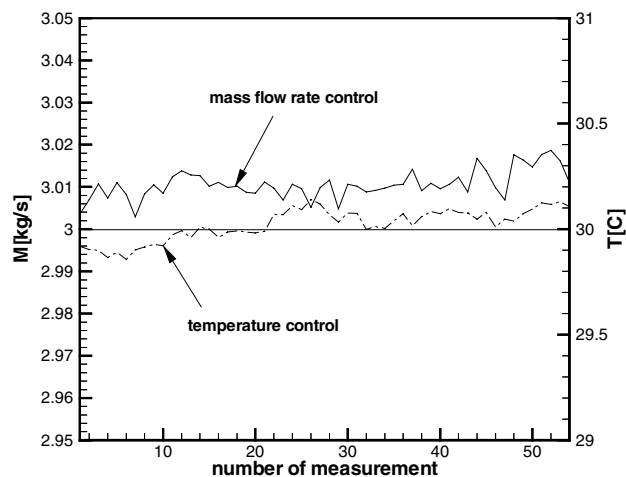

Figure 4. The control of mass flow rate and temperature in the loop water during the measurement for M=3kg/s at Z=300mm

The calming length is about 717.6mm long and sits on the top of test section. It is placed for the flow from the circular pipe to rectangular channel to be fully developed before the test section. It has the same dimension of cross-sectional area with test section. The velocity at the calming length region is measured at the cross-sectional area of half channel due to the geometric
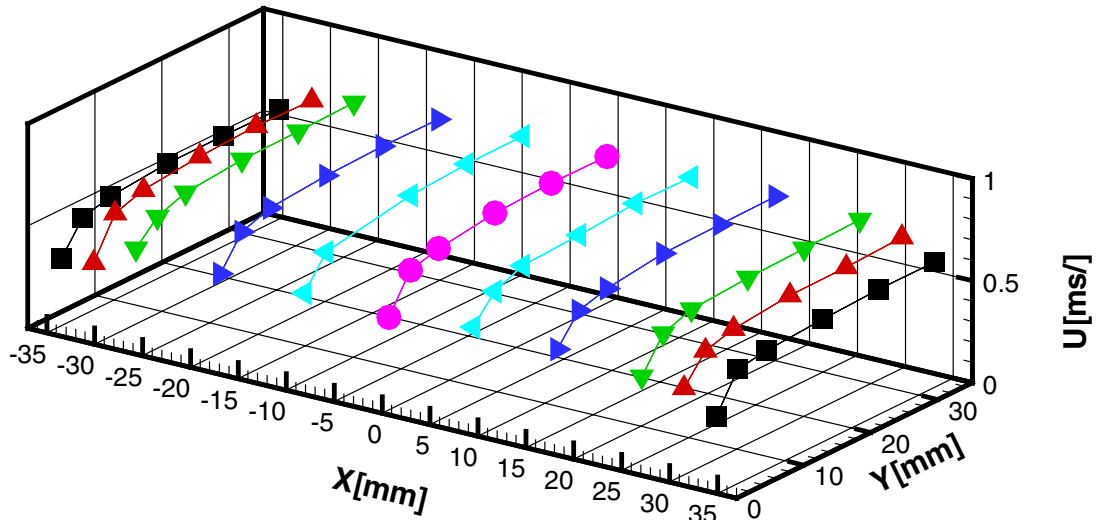
Figure 5. The velocity profile at the calming length at Z=700mm for M=3.0kg/s.

symmetry: X= -34.2, -30.8, -26.4, -17.6, -8.8, 0.0, 8.8, 17.6, 26.4, 30.8, 34.2 mm, and Y=1.0, 4.2, 8.4, 16.8, 25.2, 33.5mm from the front wall, at Z=725mm approximately 100mm above the tip of fuel plates. Here only half of front cross-sectional area of channel is measured by LDV because the too much reflection light causes difficult velocity measurement at the half of back area of channel in Y-direction. It is shown in Figure 5 that the velocity is nearly uniform in core-region of flow channel. However, the velocity decreases significantly near the wall due to the viscous effect from the wall plate. Also, the velocity field is fairly symmetric in X direction. Thus, it is assumed that the flow at the calming length from the circular pipe at the top to the rectangular channel is nearly uniform except the region near the wall even though the symmetric velocity profile is not verified in Y direction by the velocity measurement.

The velocity is measured at only a quarter cross-sectional area in the subchannels due to the complete geometric symmetry. Here the velocity is measured only at the center of each subchannel and averaged for 1000 data points. However, it should be verify the symmetry of velocity profile through the 1st to 17th subchannel. The Figure 6 shows the velocity at Y=6mm and 33.5mm, and at Z=300mm (nearly vertical center of test section) for M= 3kg/s and 5kg/s as a function of subchannel number. The velocities across the subchannels are fairly symmetric as a center of 9th subchannel except the 3rd channel. The velocity at 1st and 17th channel flow near the wall is relatively low compared with that at the central subchannels. It may be because the lower velocity from the wall frictional resistance at the calming length induces the lower mass flow entering the subchannels at the outmost subchannels: 1st and 17th subchannels. The

velocity at 9th subchannel is also slightly lower because the handle blocks the whole cross-sectional flow area above the fuel element. It may cause the lower mass flow to enter 9th subchannel. However, the velocity at 3rd channel is comparatively lower than that at 15th channel even though they are geometrically same. It is probably because of the perpendicular streamline change in the circular tube before the calming length region. To analyze this more precisely, the flow visualization will be conducted in the region of upstream at the test section. The velocities except 1st, 3rd, 9th, and 17th subchannels show nearly flat profile because of nearly uniform velocity profile developed at the core region of calming length. Therefore, the velocity profile through the subchannels can be assumed nearly symmetric through the channels of 1st to 17th. Therefore the velocity at only half of 17 subchannels (1st to 9th subchannels) is measured.
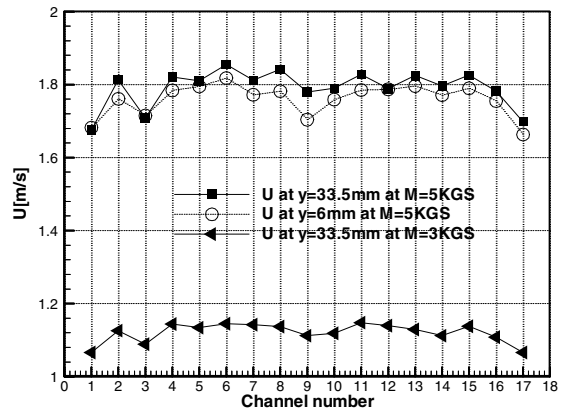

Figure 6. The symmetry in the velocity profile along the channels at Y=6mm and 33.5mm for M=3kg/s and 5kg/s.

Figure 7 shows the vertical comparison of velocity profile along the subchannel in Z-direction at 1st, 3rd, 5th and 9th subchannels. The velocity is measured vertically at Z=300mm and 1mm for different mass flow rate at each subchannel. The flow may be fully developed hydraulically at Z=300mm because the length for fully developed flow needs approximately $L_e/D_h \approx 15\sim20$; in present case, $L_e \approx 85\sim114mm$ and Z=511~540mm. at Z=300mm, the velocity near the sidewall region (Y=0~3mm) is slightly decreased by three-wall frictional resistance in comparison with that around the central region of rectangular subchannel (Y=10~33.5mm). The velocity near the central region is approximately constant due to the relatively constant frictional resistance probably from only two walls of fuel plates. This is consistent result compared with the velocity field as shown in Figure 11 in appendix. The calculated and measured velocity in rectangular channel with large aspect ratio shows that the axial velocity is relatively constant in the core-region of channel; approximately flattened cosine function shape of axial velocity profile. From the comparison of velocities at Z=300mm and at Z=1mm, mostly the velocity near the corner is slightly decreased about by 3~10% while that in the core region is increased by 2~8%. However, it is not significant variation in velocity due to the end-fitting snout. Here, it should be noted that the dotted line in each graph denotes approximate location of snout circular pipe: left side is closed by the transition piece while right side is open to the circular pipe directly. The transition piece is located by 51.8mm below the tip of fuel plates. In summary, the velocity field in a single channel is fairly uniform except corner, where the velocity is decreased by the frictional flow resistance by three sidewalls. It is consistent with axial velocity profile in rectangular channel with large aspect ratio. The velocity profile near the tip of fuel plates is slightly distorted due to the effect of exit loss. However, the velocity near the wall is retarded while that directly above the region of circular pipe is accelerated. Generally this phenomenon is observed clearly as the mass flow rate is increased. The influence of end-fitting plate, transition piece, is not significant on the vertical variation of velocity profile.
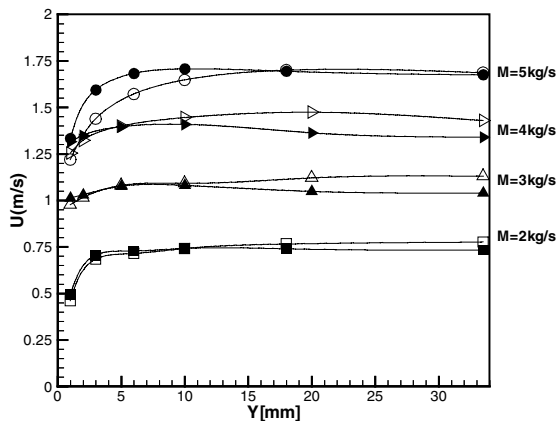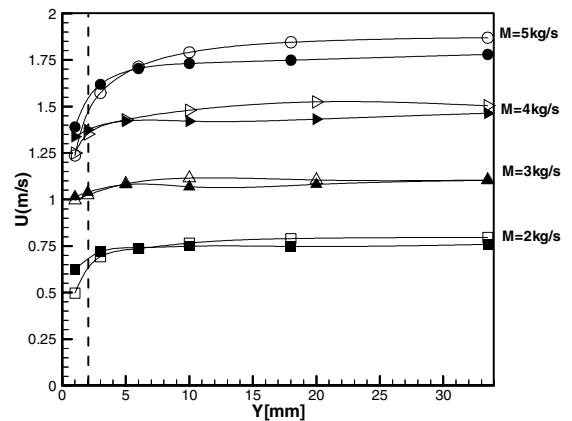

(a) 1st subchannel
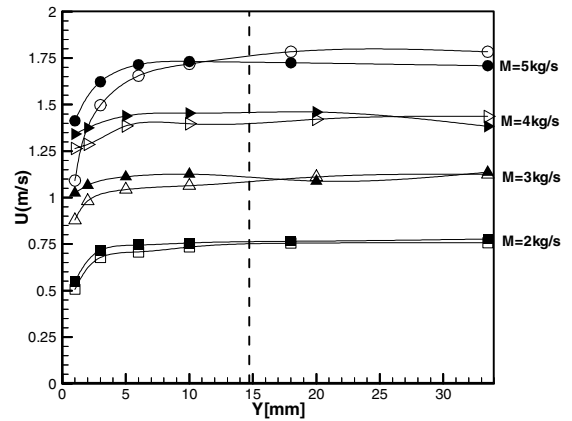
(b) 3rd subchannel
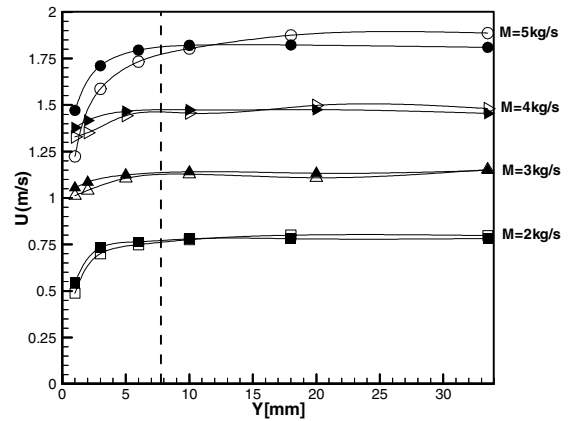
(c) 5th subchannel

(d) 9th subchannel

Figure 7. The velocity profile at different channels at Z=300mm and 1mm for the different mass flow rate: solid symbol at Z=300mm & hollow symbol: z=1mm. The dotted line denotes the location of circumferential line of end-fitting snout.

The velocities at 6 different locations at each channel at Z=300mm and 1mm are averaged by equation (1).

$$u_{mean} = \frac{\sum_i A_i u_i}{A_i} \qquad (1)$$

where u_i is the local velocity at measurement point and A_i is the cross-sectional area around that u_i. At the cross-sectional area A_i, the velocity is assumed uniform in X-direction around u_i. The average mass flow rate is calculated by $M = \rho u_{mean} A$ where fluid density is evaluated at 30°C, and A is the cross-sectional area of single subchannel. Figure 8 shows the mass flow rate in each subchannel. The flow rate is distributed fairly well through 1st to 9th subchannel. To investigate the mass flow rate fraction, the mass flow rate distribution is plotted in Figure 9. It is clearly shown that mass flow is distributed very well through the subchannels. Only the deviation is within ±5%. In order to compare this experimental result with numerical calculation, the mass flow distribution from Blahnik's calculation is shown in Figure 10 in appendix as well as the result of Rummen's experiment in Figure 9. For the case of M=1.2kg/s, the experimental result of Rummens' and numerical calculation of Blahnik's shows a consistent result. The flow rate fraction at 1st, 2nd, 16th and 17th subchannels is fairly low: approximately 80~95% of subchannels' average while that from 4th to 15th subchannels is slightly higher than the subchannels' average. It is reasonable because the subchannels in the central region have more cross-sectional area of element open to the flow region in snout. Thus, the exit loss from the flow stream change is much lower than at the outmost subchannels. Also, the mass flow fraction from 9th to 15th subchannels is slightly higher than that from 4th to 8th subchannels because the more cross-sectional area open to flow region in snout. However, for the case of M=5.0kg/s, the present result shows extremely uniform distribution of mass flow through the subchannels compared with numerical calculation. It might be because of over-estimation of exit loss in numerical calculation or the difference of real curved 18-plate fuel element and simulated flat 18-plate fuel element. The exit loss in present fuel element may consist of two factors: flow area expansion, and gradual flow area contraction at the transition piece from rectangular channel to circular pipe and flow stream change[6][7]. The exit loss coefficient K for flow area expansion can be calculated K=0.508. However, the cross-sectional area of fuel plate is so small in the width of 1.27mm that the eddy structure may not be able to develop fully. Also, the exit loss of gradual area contraction and flow stream change occurs downstream approximately 51.8mm below from the tip of fuel plate. Therefore it may not influence the directly velocity because the velocity is measured upstream at Z=1mm. Therefore, the exit loss may be over-estimated for numerical calculation in both cases of flow area expansion, and gradual flow area contraction and flow stream change. On the other hand, the geometrical difference between the real fuel element and simulated one may influence the mass flow distribution because the fuel plate shape is different and the cross-sectional area blocked by end-fitting snout is different. The blocked cross-sectional area by snout in the simulated fuel element is larger in the first 8 subchannels (1st to 8th) and smaller in last 8 subchannels (10th to 17th) than that in real one. From the comparison of Rummens' experimental result of M=1.2kg/s and present experiment, the effect by curve-fuel plate must be considered for general shape of mass flow distribution. In order to investigate the effect of cured fuel plate more in detail, the experiment must be conducted for M=1.2kg/s with simulated 18-plate fuel element and compare both results. In summary, the mass flow in simulated fuel element shows fairly uniform distribution through the subchannels. It is not consistent with result of experimental result of M=1.2kg/s and numerical calculation.

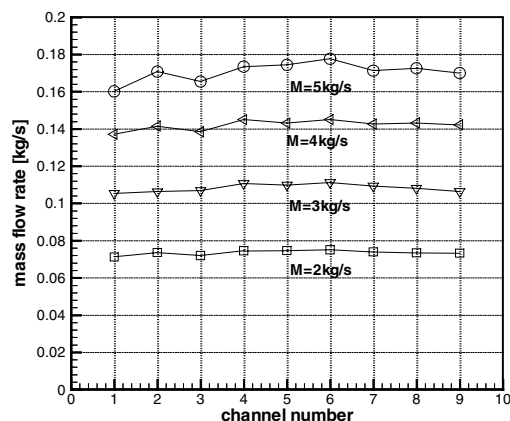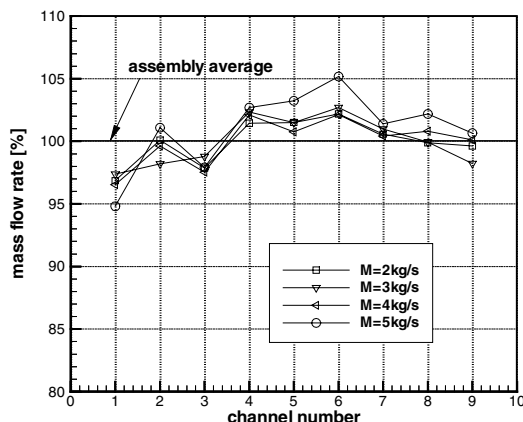Figure 8. The mass flow rate profile in the 18-plate fuel channels for M=2.0, 3.0, 4.0, and 5kg/s

Figure 8. The mass flow rate fraction in the 18-plate fuel channels for M=2.0, 3.0, 4.0, and 5kg/s

4. Conclusion

The flow velocity at the simulated 18-plate fuel element of McMaster Nuclear Reactor is measured by LDV for the range of M=2.0kg/s to 5.0kg/s in order to obtain the mass flow distribution through the subchannels.

1. The velocity measurement at the calming length region shows that fairly uniform velocity field is developed before the test section. Also, it is shown from the 17 channel flow measurement that the velocity as a center of 9th channel is very symmetric due to the geometrical symmetry.

2. The velocity profile at the fully developed region has the flattened cosine function shape. The vertical variation in the velocity profile is not significant due to the exit loss. The effect of exit end-fitting is not significant in the present experiment.

3. The mass flow rate is fairly well distributed from 1st to 9th subchannels. The mass flow fraction at outmost subchannels (1st to 2nd subchannels) is approximately within 95~97% of average subchannel mass flow rate. Also mass flow fraction at the center channel (9th) is slightly lower than that at the other subchannels due to the handle blockage effect. The highest mass flow fraction is detected from 4th to 7th channels. The measured mass flow distribution is fairly more uniform through the channels in comparison with result of numerical calculation,.

5. Concluding Remarks

The velocity measurement through the channels is conducted for only 4 mass flow rate (M=2.0, 3.0, 4.0, 5.0kg/s) for the present. For more accurate analysis, the velocity measurement will be conducted by varying flow rate by the increase of 0.25 or 0.5kg/s. The flow visualization will be performed to understand the exit end-fitting effect more clearly in the transitional region of rectangular channel to circular pipe. In addition, the velocity at the real curved 18-plate fuel element will be numerically calculated, and the velocity profile both at the curved fuel element and at the flat fuel element will be compared to investigate the effect of curved plate on the velocity.
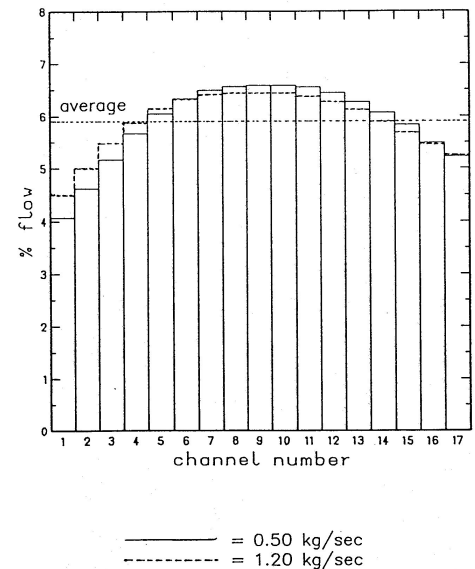
6. Appendix

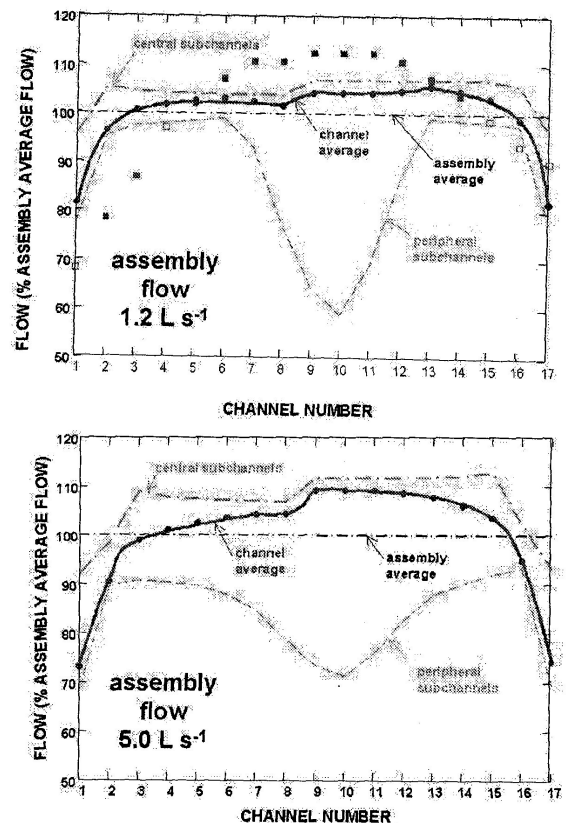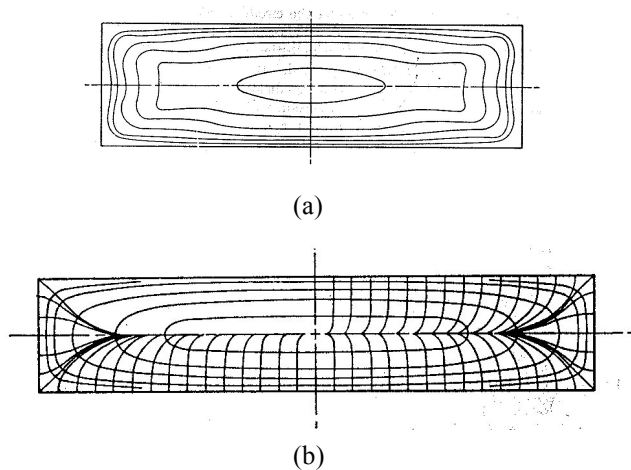Figure 9. Flow distribution among channels of 18-plate element from H. Rummens' work [3].

Figure 10. Flow distribution among channels of 18-plate element from the calculation of by C. Blahnik[1].

(a)

(b)

Figure 11. (a) experimental velocity distribution of aspect ratio A=3.5:1 rectangular duct [9] and (b) computed velocity distribution of aspect ratio A=5.0:1 rectangular duct [9]

7. Reference

1. C. Blahnik, " Draft document of current MNR safety report", May 30, 2000.
2. H.E.C. Rummens, "Thermalhydraulic Studies of the McMaster Nuclear Core", McMaster University, Master's Thesis, 1988.
3. Wm. J. Garland, "Thermalhydraulic Modeling of the McMaster Nuclear Reactor", MNR Technical Report 97-04, 1997.
4. S. I. Osamusali, "Development of the McMaster Nuclear Reactor Thermalhydraulic Simulation Loop", McMaster University, Master's Thesis, 1985.
5. I. E. Idelchik, "Handbook of Hydraulic Resistance", 2nd Edition, Hemisphere Publishing Corp., 1986.
6. R.D. Blevins, "Applied fluid dynamic handbook", N.Y. Van Nostrand Reinhold Co., 1984.
7. F. M. White, "Fluid Mechanics", 2nd Edition, New-York McGraw-Hill Book Co. INC, 1994.
8. J. P. Hartnett, J.C.Y. Koh, and S.T. McComas, "A comparison of predicted and measured friction factors for turbulent flow through rectangular ducts", J. of Heat Transfer, pp. 82-88, 1962,
9. R. W, Hanks, "On the theoretical calculation of friction factors for laminar, transitional, and turbulent flow of Newtonian fluids in pipes and between parallel plane walls", J. AIChE, vol. 14, No. 5, pp. 691-695, 1968.